

Reaction of the Nitrate Radical with Some Potential Automotive Fuel Additives. A Kinetic and Mechanistic Study

Sarka Langer* and Evert Ljungström

Department of Inorganic Chemistry, University of Göteborg, S-412 96 Göteborg, Sweden

Received: November 29, 1993; In Final Form: February 23, 1994*

Rate coefficients for the reaction of NO_3 with ethyl *tert*-butyl ether (ETBE), diisopropyl ether (DIPE), and *tert*-amyl methyl ether (TAME) have been determined. Absolute rates were measured at temperatures between 257 and 367 K using the fast flow–discharge (FFD) technique. Relative rate experiments were also performed at 295 K in a reactor equipped with White optics and using FTIR spectroscopy to follow the reactions. Rate data from FFD experiments can be presented as follows: $k_{\text{ETBE}} = (2.48 \pm 0.78) \times 10^{-12} \exp[-(1613 \pm 542)/T]$, $k_{\text{DIPE}} = (2.02 \pm 0.35) \times 10^{-12} \exp[-(1759 \pm 301)/T]$, and $k_{\text{TAME}} = (1.21 \pm 0.22) \times 10^{-12} \exp[-(1874 \pm 304)/T]$ (in units of $\text{cm}^3 \text{ molecule}^{-1} \text{ s}^{-1}$). The rate coefficients at room temperature from the FFD experiments are in good agreement with the corresponding rate coefficients from the relative rate experiments. Products from simulated atmospheric oxidation of the investigated ethers, initiated by the reaction with the nitrate radical, were identified using FTIR spectroscopy. The degradation of ETBE results in *tert*-butyl formate, *tert*-butyl acetate, formaldehyde, and methyl nitrate, that of DIPE in acetone, isopropyl nitrate, isopropyl acetate, and formaldehyde, and that of TAME in *tert*-amyl formate, formaldehyde, and *tert*-amyl nitrate.

Introduction

Currently, a large research effort within the petroleum industry is devoted to develop new, more “environment-friendly” fuel formulations. A number of oxygen-containing compounds such as alcohols and ethers have been proposed as fuel additives. A highly branched ether, methyl *tert*-butyl ether (MTBE), is already used as a component of such formulations. Addition of MTBE to gasoline reduces the CO emissions and increases the octane rating, thereby making the use of alkyl lead compounds unnecessary.¹ In addition to MTBE, ethyl *tert*-butyl ether (ETBE), diisopropyl ether (DIPE), and *tert*-amyl methyl ether (TAME) have been proposed for exploration.^{1,2} All these compounds have a comparatively high volatility, which makes their possible use as automotive fuel additives a potential source of large emissions to the atmosphere. Investigations of kinetics and mechanisms of the atmospheric oxidation of ETBE, DIPE, and TAME by OH radicals have recently been published.^{3–6} Reaction with the hydroxyl radical is the main atmospheric route for destruction of ethers during daytime since photolysis⁷ and reaction with ozone⁸ are expected to be negligibly slow. Products of atmospheric OH-initiated oxidation are mainly the corresponding esters and carbonyl group-containing smaller organic compounds.

In Scandinavia, the dark periods of a year are significant and, therefore, sink processes other than reaction with OH may be important for ethers. One possible process is reaction with the nitrate radical. Nitrate radicals are formed from the reaction between ozone and nitrogen dioxide. This radical species is present in the atmosphere in significant concentrations only during dark conditions owing to its rapid photolysis by visible light. The reaction of nitrate radicals with aliphatic ethers has not received much attention, probably due to the expected inertness of such ethers to this reactant. Recently, however, rates of reaction between the nitrate radical and dimethyl ether, diethyl ether, di-*n*-propyl ether, and MTBE in a temperature range from 258 to 373 K have been measured in our laboratory.⁹ The reaction proceeds *via* hydrogen atom abstraction, forming nitric acid and other products. The rate coefficients are remarkably large even when the influence of the –O– ether group on adjacent C–H bonds is taken into account.

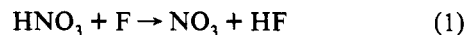
Here we report the rate coefficients for gas-phase reaction of

ethyl *tert*-butyl ether (ETBE), diisopropyl ether (DIPE), and *tert*-amyl methyl ether (TAME) with the nitrate radical in a temperature range between 257 and 367 K. The reaction products under simulated atmospheric conditions are also presented.

Experimental Setup and Procedures

A fast flow–discharge (FFD) apparatus was used to measure absolute rate coefficients and temperature dependencies. Relative rates (RR) and reaction products were measured using a batch reactor and FTIR spectroscopy.

The setup and procedures related to the FFD experiments have been described in some detail earlier,¹⁰ and only a brief description will be given here. The apparatus is of a conventional type with an axially moveable injector for the organic compound in order to obtain time resolution. Helium was used as the carrier gas. Nitrate radicals were generated according to (1) by reaction of fluorine atoms from a microwave discharge with an excess of nitric acid. The nitrate radicals were detected by optical



absorption at 662 nm using a multipass cuvette with a total path length of 72 cm. A modulation technique with lock-in detection was employed to observe small changes in transmittance. The practical nitrate radical detection limit with this system is approximately $5 \times 10^{11} \text{ molecule cm}^{-3}$. To reach high enough concentrations of the ethers, liquid at normal temperature and pressure, they were delivered as vapor to the flow tube injector from a classical low-pressure distillation apparatus.

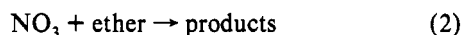
All FFD experiments were performed under pseudo-first-order conditions. The measured quantities were the change in transmittance signal when NO_3 was added to the system as compared to the case when no NO_3 was produced, Δ_{NO_3} , and the change in signal when both NO_3 and the organic substance were added, $\Delta_{\text{NO}_3+\text{org}}$, as a function of reaction time t . For pseudo-first-order conditions and small absorbances, it can be shown that equation (I) holds. The first-order rate coefficients k' were obtained from

$$\ln(\Delta_{\text{NO}_3}/\Delta_{\text{NO}_3+\text{org}}) = k't \quad (I)$$

least-squares straight lines according to eq I, and the desired rate coefficient k , for reaction 2 as defined by eqs II and III, was

* Abstract published in *Advance ACS Abstracts*, May 1, 1994.

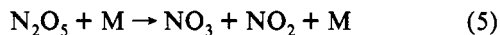
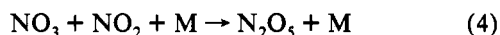
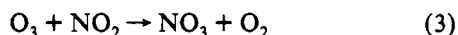
determined from similar fits of k' vs [ether].



$$d[\text{NO}_3]/dt = -k[\text{NO}_3][\text{ether}] \quad (\text{II})$$

$$k' = k[\text{ether}] \quad (\text{III})$$

A detailed description of the experimental setup for the relative rate experiments was given by Wängberg et al.¹¹ The reaction chamber has a volume of 153 L and is equipped with a 2-m base-path White optical system which is connected to a Mattson Polaris FTIR spectrophotometer equipped with an MCT detector. An optical path length of 40 m and a spectral resolution of 1 cm⁻¹ were used in all experiments. The reagents were metered by volume–pressure measurements and were introduced into the reactor from a vacuum line. The bath gas was mixed so as to obtain 20% O₂ in N₂ at the experimental pressure of 1000 mbar. The relative rate experiments were made at 295 K. Nitrate radicals were generated by thermal decomposition of N₂O₅ which, in turn, was prepared *in situ* by reaction of O₃ with an excess of NO₂ according to reactions 3–5. An ether and a reference



compound were added to the reaction chamber to give between 2.5 and 5 × 10¹⁴ molecule cm⁻³ of each in the presence of between 2 and 6 × 10¹⁴ molecule cm⁻³ of N₂O₅. The reaction was then followed for several hours. The nitrate radicals react with the ether and with the reference compound according to reactions 2 and 6.



It has been shown¹² that eq IV describes the loss of organic compounds. Subscripts 0 and t indicate concentration at the

$$\ln([\text{ether}]_0/[\text{ether}]_t) = (k_{\text{ether}}/k_{\text{ref}})\ln([\text{ref}]_0/[\text{ref}]_t) \quad (\text{IV})$$

beginning of an experiment and a time t , respectively. It should be noted that, since the concentrations are used as a ratio, any quantity proportional to the concentration could be used instead of the absolute concentration. The desired rate coefficient was obtained from the slope of a plot of $\ln([\text{ref}]_0/[\text{ref}]_t)$ vs $\ln([\text{ether}]_0/[\text{ether}]_t)$ and a literature value of the rate coefficient of the reference compound. Secondary reactions involving nitrate radicals are of no consequence for this type of determination unless products or N₂O₅ attack the original organic materials. Two reference compounds were used for each of the investigated compounds in order to check the internal consistency of the determined rate coefficients. The investigated compound and the reference should react with the nitrate radical at rates comparable within an order of magnitude, and both should have well-developed and well-positioned IR absorption bands to make the evaluation accurate. In order to fulfil the above-mentioned conditions, 3-chloro-1-butene ($k_{\text{NO}_3} = (2.8 \pm 0.7) \times 10^{-15}$ cm³ molecule⁻¹ s⁻¹)¹³ and propene ($k_{\text{NO}_3} = (9.5 \pm 2.1) \times 10^{-15}$ cm³ molecule⁻¹ s⁻¹)¹⁴ were used as references in our RR experiments.

Reaction product studies were conducted with the same equipment and under the same conditions as the relative rate experiments. Ether and N₂O₅ were added into the reaction chamber in concentrations between 2.5 × 10¹⁴ and 4 × 10¹⁴ molecule cm⁻³, and reactions were followed by FTIR spectroscopy until almost all of the N₂O₅ was consumed. Then NO was added

TABLE 1: IR Absorption Coefficients at 1 cm⁻¹ Spectral Resolution at 1000 mbar and 295 K

compd	ν/cm^{-1}	$\sigma/\text{cm}^2 \text{ molecule}^{-1}$ (base 10)	range ^a
ETBE	1083	$(2.17 \pm 0.07) \times 10^{-19}$	<0.30
DIPE	1021	$(1.83 \pm 0.07) \times 10^{-19}$	<0.40
TAME	1096	$(2.67 \pm 0.01) \times 10^{-19}$	<0.30
3-chloro-1-butene	714	$(6.99 \pm 0.27) \times 10^{-20}$	<0.20
propene	912	$(2.43 \pm 0.02) \times 10^{-19}$	<0.50
HCHO ¹⁵	1746	$(3.50 \pm 0.08) \times 10^{-19}$	<0.20
isopropyl acetate	1758.8	$(5.93 \pm 0.16) \times 10^{-19}$	<0.43
<i>tert</i> -butyl acetate	1758.6	$(5.91 \pm 0.16) \times 10^{-19}$	<0.40
<i>tert</i> -butyl formate	1744	$(1.29 \pm 0.04) \times 10^{-18}$	<0.50
<i>tert</i> -amyl formate	1743	$(1.34 \pm 0.02) \times 10^{-18}$	<0.50
RONO ¹⁵	≈1660	$(1.8 \pm 0.4) \times 10^{-18}$	<0.30
methyl nitrate	855	$(3.79 \pm 0.09) \times 10^{-18}$	<0.20
acetone	1739	$(2.10 \pm 0.11) \times 10^{-19}$	<0.50

^a Range denotes the linear absorbance interval.

TABLE 2: Experimental Conditions Employed in the Fast Flow–Discharge Experiments for the Investigation of the Reaction of NO₃ with ETBE, DIPP, and TAME between 257 and 367 K^a

compd	p^b/mbar	[ether] ^c /10 ¹⁵ molecule cm ⁻³	$v^d/\text{cm s}^{-1}$
ETBE	3.4–3.8	0.23–1.41	720–1100
DIPE	3.3–3.7	0.28–2.28	720–1140
TAME	3.2–4.1	0.36–3.57	500–1050

^a $[\text{NO}_3]_0 \leq 1.5 \times 10^{13}$ molecule cm⁻³. ^b p is the range of experimental pressures covered. ^c [ether] is the range of ether concentrations. ^d v is the range of linear flow velocities in the flow tube.

to the mixture to transfer any remaining alkylperoxy compounds into products.

Reference spectra of pure compounds at known concentration were subtracted from the observed product spectra to quantify products. The linearity between absorption and concentration was confirmed by separate calibrations for all compounds employed in both relative rate and product studies. Wavenumbers and the corresponding absorption coefficients, originating from “in house” calibrations, used in the evaluation are summarized in Table 1. References of organic nitrates other than methyl nitrate were not prepared, and a mean value of published absorption coefficients¹⁵ has been used to calculate yields of organic nitrates (RONO₂) in our experiments.

The following chemicals were used: ETBE >97% (Fluka), DIPE >99% (Fluka), TAME >94% (Aldrich), 3-chloro-1-butene >98% (Merck), propene >99.8% (AGA Gas AB), *tert*-butyl formate >99% (Aldrich), *tert*-butyl acetate >99% (Merck), isopropyl acetate >99% (Merck), helium 99.9995%, nitrogen ≥99.995%, oxygen ≥99.995%, nitrogen dioxide 3% in nitrogen (all gases AGA Gas AB). *tert*-Amyl formate was synthesized according to Barkenbus et al.,¹⁶ and the identity and purity of the compound was checked by ¹H NMR. All ethers and esters were subjected to repeated freeze–pump–thaw cycles, and 3-chloro-1-butene was freshly distilled before use. Propene was used as received.

Results and Discussion

The rate coefficients presented in this work are the first determinations for reaction between NO₃ radicals and ETBE, DIPE, and TAME.

Fast Flow–Discharge Experiments. Some experimental information is summarized in Table 2. Figure 1 shows the pseudo-first-order plots, and Figure 2 shows the corresponding second-order plot from a typical run with ETBE and NO₃ at 324 K. The second-order straight line has an intercept of 1.71 ± 0.72 s⁻¹. This behavior is observed in all second-order plots and is the result of wall losses of NO₃. Values of the observed rate coefficients at various temperatures are summarized in Table 3.

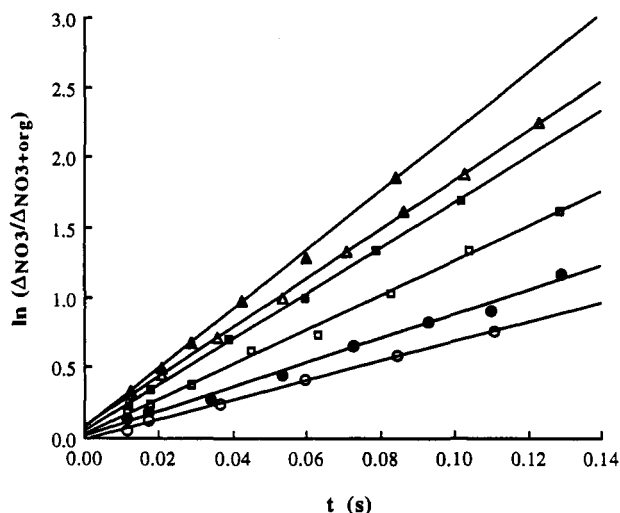


Figure 1. Experimental data from the fast flow-discharge experiments. Pseudo-first-order plots for various concentrations of ethyl *tert*-butyl ether at 324 K. Open circles, 2.92×10^{14} ; filled circles, 3.89×10^{14} ; open squares, 5.51×10^{14} ; filled squares, 7.94×10^{14} ; open triangles, 9.06×10^{14} ; filled triangles, 10.41×10^{14} (in molecule cm^{-3}).

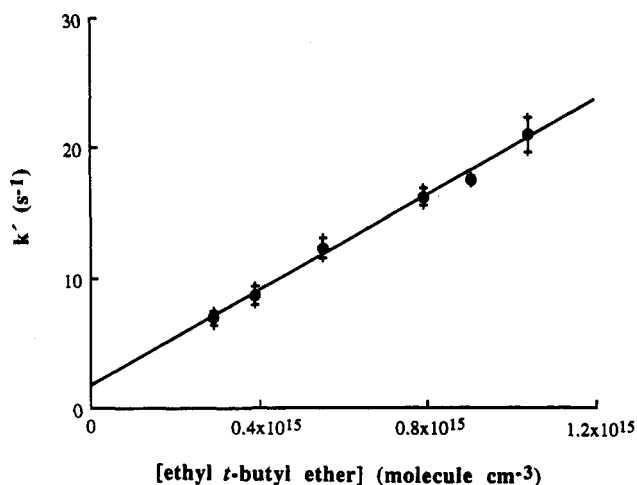


Figure 2. Plot of pseudo-first-order rate coefficients vs. concentration of ethyl *tert*-butyl ether at 324 K, $p_{\text{exp}} = 3.5$ mbar.

TABLE 3: Rate Coefficients for the Reaction of NO_3 Radicals with ETBE, DIPE, and TAME Determined in the Fast Flow-Discharge Experiments^a

T	k_{ETBE}	T	k_{DIPE}	T	k_{TAME}
257	5.08 ± 2.82	257	2.00 ± 0.65	257	0.79 ± 0.27
		273	3.54 ± 1.66		
295	8.71 ± 2.26	295	5.18 ± 0.98	295	2.02 ± 0.49
324	18.24 ± 2.26	323	9.10 ± 2.68	324	3.87 ± 1.08
348	21.50 ± 6.57	344	10.41 ± 3.35	348	4.74 ± 1.44
363	32.87 ± 3.11	364	17.39 ± 6.31	367	7.43 ± 2.16

^a The errors represent the 95% confidence interval. Temperatures (T) in K. All k values are reported in units of $10^{-15} \text{ cm}^3 \text{ molecule}^{-1} \text{ s}^{-1}$.

Determination of small rate coefficients such as those presented here is quite sensitive to side reactions especially if only one of the reactants is measured. In our previous work,⁹ we did not, however, observe any influence of secondary reactions on ether rate coefficients. In cases where secondary reactions may be suspected, it is good practice to validate the results by an independent technique. In our case, this was made by the relative rate experiments discussed below.

Arrhenius plots derived from the observed rate coefficients can be seen in Figure 3. The straight lines drawn in this figure represent the following Arrhenius expressions (error limits are the 95% confidence interval, and k values are reported in units

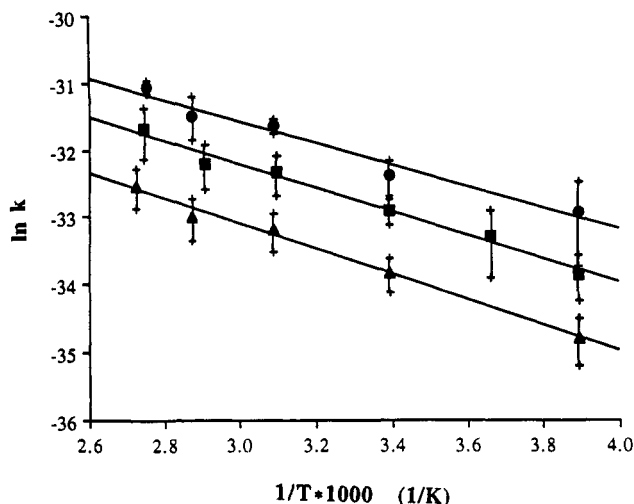


Figure 3. Arrhenius plots for the reaction of the NO_3 radical with ethyl *tert*-butyl ether (circles), diisopropyl ether (squares), and *tert*-amyl methyl ether (triangles). The lines correspond to the Arrhenius equations given in the text.

TABLE 4: Results of the Relative Rate Experiments. The Experiments Were Made in Synthetic Air at 295 K and at a Pressure of 1000 mbar^a

ether	3-chloro-1-butene		propene	
	$k_{\text{ether}}/k_{\text{ref}}$	k_{ether}	$k_{\text{ether}}/k_{\text{ref}}$	k_{ether}
ETBE	3.55 ± 0.28	9.94 ± 3.27	0.99 ± 0.06	9.31 ± 2.60
DIPE	1.84 ± 0.18	5.15 ± 1.81	0.53 ± 0.02	5.04 ± 1.26
TAME	0.91 ± 0.14	2.54 ± 1.03	0.21 ± 0.01	1.97 ± 0.53

^a k_{ether} was obtained from the slope of the line defined by eq IV and the reference rate coefficient, k_{ref} . 3-chloro-1-butene: $k_{\text{NO}_3} = (2.8 \pm 0.7) \times 10^{-15}$ (ref 13). propene: $k_{\text{NO}_3} = (9.5 \pm 2.1) \times 10^{-15}$ (ref 14). All k in the table are reported in units of $10^{-15} \text{ cm}^3 \text{ molecule}^{-1} \text{ s}^{-1}$.

of $\text{cm}^3 \text{ molecule}^{-1} \text{ s}^{-1}$):

$$\text{ETBE} \quad k = (2.48 \pm 0.78) \times 10^{-12} \exp[-(1613 \pm 542)/T]$$

$$\text{DIPE} \quad k = (2.02 \pm 0.35) \times 10^{-12} \exp[-(1759 \pm 301)/T]$$

$$\text{TAME} \quad k = (1.21 \pm 0.22) \times 10^{-12} \exp[-(1874 \pm 304)/T]$$

The corresponding activation energies are (in units of kJ mol^{-1}) 13.4 ± 4.5 , 14.6 ± 2.5 , and 15.6 ± 2.5 for ETBE, DIPE, and TAME, respectively. The activation energy values are consistent with those for aliphatic ethers found earlier⁹ and confirm the expected hydrogen atom abstraction reaction mechanism.

Relative Rate Experiments. A set of relative rate experiments was performed to confirm the validity of the FFD determinations. The results are shown in Table 4. The relative rate experiments rely on the observation of the concentration decrease of the organic compound of interest relative to a reference substance in the presence of nitrate radicals. The relative rate experiments were carried out at atmospheric pressure in synthetic air and at room temperature. The reaction of NO_3 radicals with organic compounds in the presence of oxygen gives rise to organic peroxy radicals (RO_2) and HO_2 . The subsequent chemistry of these radicals is complex, but they are not expected to react extensively with any of the investigated or reference organic substances used in this work. Figure 4 is an example of plots used to evaluate the relative rate experiments. The slopes of the lines in Figure 4, $k_{\text{ether}}/k_{\text{ref}}$, combined with literature values of k_{ref} give the desired value of k_{ether} . The errors of the relative rate coefficients are derived from the slope of the plot according to eq IV and the errors in the reference compound rate coefficient. By comparing Table 4 with the appropriate entries in Table 3, it is clear that the rate coefficient values determined by the two methods are identical within the limits of error. This means that the FFD

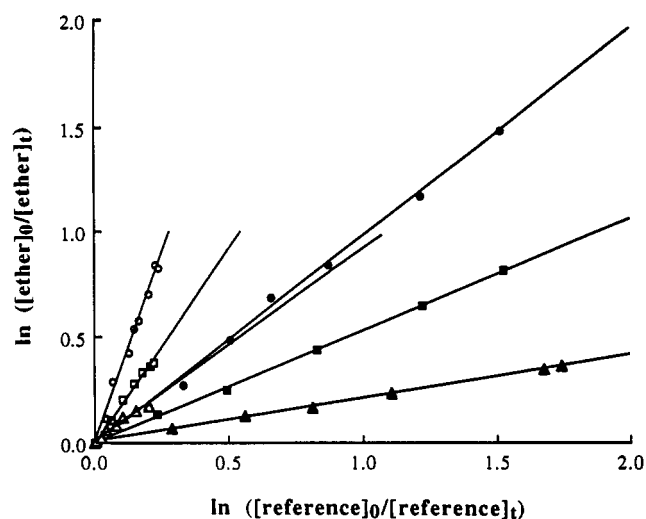


Figure 4. Experimental data from the relative rate experiments with ethyl *tert*-butyl ether (circles), diisopropyl ether (squares), and *tert*-amyl methyl ether (triangles). Filled symbols, propene as the reference compound; empty symbols, 3-chloro-1-butene as the reference compound.

data are free from noticeable influence from secondary reactions and that the assumed 1:1 stoichiometry is confirmed. In addition, the initial abstraction step is identical at low pressure in helium and in air at atmospheric pressure. The FFD-derived kinetic data are therefore expected to describe, with good accuracy, ether- NO_3 reactions in the atmosphere.

Reaction Products. Experiments to investigate the atmospheric degradation of ETBE, DIPE, and TAME, initiated by attack of the NO_3 radical, were conducted. NO_3 radicals were generated by thermal decomposition of N_2O_5 in the same way as for the relative rate experiments. This procedure involves quite large concentrations of NO_2 , present in the reaction mixture, which can react with, e.g., peroxy radicals, formed in previous reaction steps, to form moderately stable peroxy nitrates. Alkoxy radicals can generally be formed from peroxy radicals by mechanisms such as self-reaction, reaction with nitrate or hydroperoxy radicals, or reaction with nitric oxide. In order to speed up the decomposition of peroxy nitrates, NO was added in excess to the reaction mixture when the concentration of N_2O_5 had decreased to zero. The absorbance of infrared bands attributed to peroxy nitrates then disappeared and the concentration of nitrogen dioxide and stable products underwent a corresponding increase.

ETBE. Atmospheric oxidation of ETBE initiated by OH and Cl radicals in the presence of NO has already been studied,^{3,4} and complex sets of products were found.

An estimate of the NO_3 reactivity with the *tert*-butyl side suggests that the abstraction occurs on the ethoxy side of ETBE. The methyl groups on the *tert*-butyl side are sufficiently screened off from the influence of the $-\text{O}-$ atom, and their contribution to the overall rate coefficient may be predicted using the correlation expression for alkanes given by Bagley et al.¹⁷ The nine abstractable hydrogen atoms on the *tert*-butyl side would contribute to the NO_3 radical rate coefficient at room temperature by $3 \times 10^{-18} \text{ cm}^3 \text{ molecule}^{-1} \text{ s}^{-1}$, representing approximately 0.03% of the overall observed rate coefficient for ETBE of $8.71 \times 10^{-15} \text{ cm}^3 \text{ molecule}^{-1} \text{ s}^{-1}$ at 295 K.

As is confirmed by the observed product distribution, the nitrate radical initiated attack does indeed take place on the ethoxy side of the molecule and the *tert*-butoxy moiety remains intact. In this experiment, 6.8 ppm of ETBE disappeared representing 40% of the initial concentration. ETBE reacted with nitrate radicals in air and in the presence of nitrogen dioxide to form *tert*-butyl formate (TBF), *tert*-butyl acetate (TBA), formaldehyde, and methyl nitrate in fractional yields of 0.71, 0.25, 0.31 and 0.34, respectively. Figure 5 shows the infrared spectrum of the products except methyl nitrate.

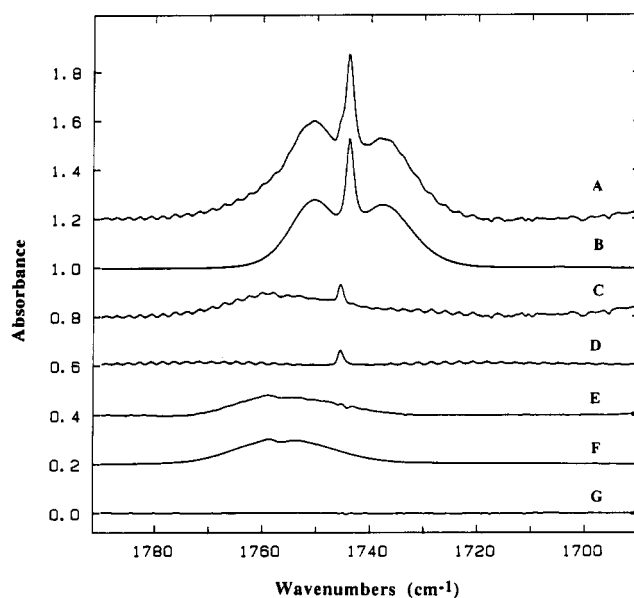


Figure 5. Identification of products from experiments with ETBE. (A) Spectrum of stable products after NO addition. (B) Reference spectrum of *tert*-butyl formate (4.8 ppm). (C) The result of the spectral subtraction of B from A. (D) Reference spectrum of formaldehyde (1.7 ppm). (E) The result of the subtraction of D from C. (F) Reference spectrum *tert*-butyl acetate (2.1 ppm). (G) The result of the subtraction of F from E.

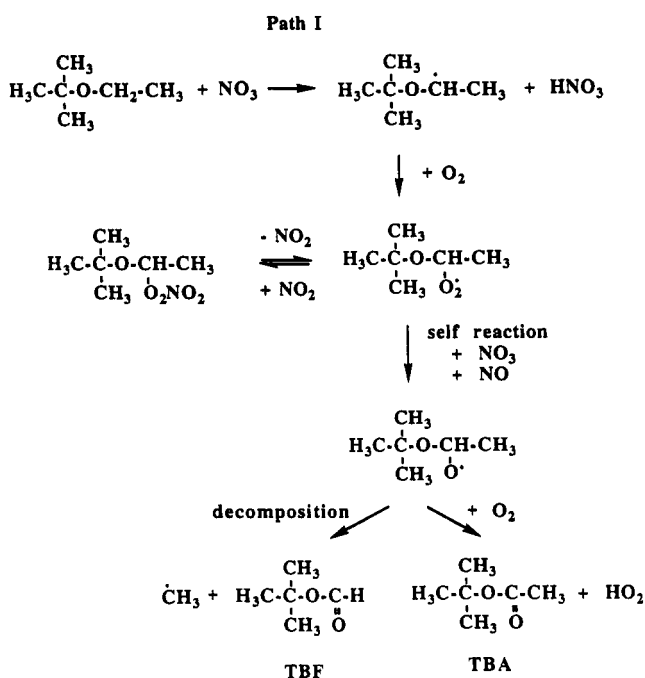


Figure 6. Reaction mechanism for the reaction of the nitrate radical with ETBE. The degradation is started by the abstraction of a secondary hydrogen atom.

Possible reactions leading to formation of the products observed in our system are given by the pathways which were originally proposed by Wallington and Japar³ and which are shown in Figures 6 and 7. Two different alkyl radicals can be formed in the first abstraction step. Path I, depicted in Figure 6, is expected to be the major pathway for TBF and the only route for TBA formation, since hydrogen atom abstraction from the secondary carbon atom is expected to dominate over abstraction from the primary positions. The alkoxy radical, formed in path I, can be removed by decomposition, resulting in TBF and a methyl radical or by reaction with O_2 , forming TBA and a hydroperoxy radical. Several of the intermediates in the reaction sequences are identical regardless of whether the initial attack was by NO_3 , OH , or Cl .

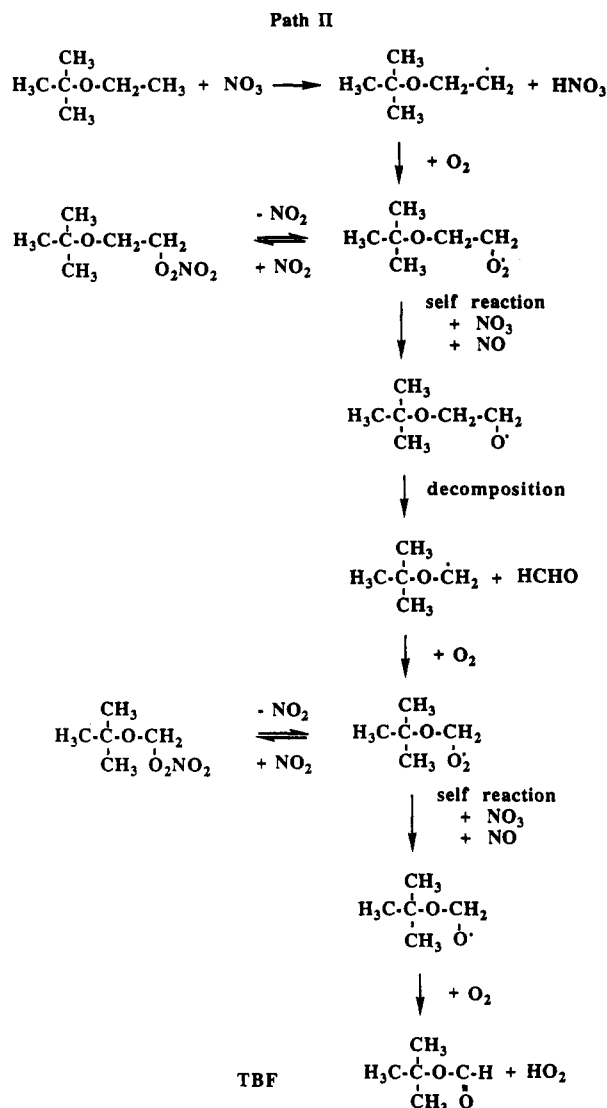


Figure 7. Reaction mechanism for the reaction of the nitrate radical with ETBE. The degradation is started by the abstraction of a primary hydrogen atom.

The formation of TBA, observed both by Smith et al.⁴ and by us, is an indication that the alkoxy radical appearing in Figure 6 is formed. The probability for hydrogen abstraction by O₂ in air or decomposition of this radical appears to be of the same order of magnitude.

Figure 7 represents the second reaction pathway where the reaction is started by abstraction of a hydrogen atom from the primary position. The alkoxy radical, formed in path II, decomposes to HCHO and a new radical. The new radical is converted by subsequent reactions into TBF and a hydroperoxy radical.

The methyl radicals generated in path I are turned into HCHO or CH₃ONO₂ via methylperoxy and methoxy radicals. Paths I and II are indistinguishable in terms of TBF and subsequent formaldehyde and methyl nitrate formation, but path I is the only way for TBA formation. Mass balance calculations show that the sum of the yields of TBF and TBA is 0.96 which is in good agreement with the theoretical value of 1.00 since each molecule of ETBE is transformed either into TBF or TBA. HCHO and CH₃ONO₂ give together a yield of 0.65 that should be the same as the fraction of TBF formed; also here, the agreement is acceptable.

Smith et al.⁴ describe another set of products, i.e., ethyl acetate, acetone, and acetaldehyde, as a result of the OH radical attack on the *tert*-butyl side of ETBE. Low yields of these compounds

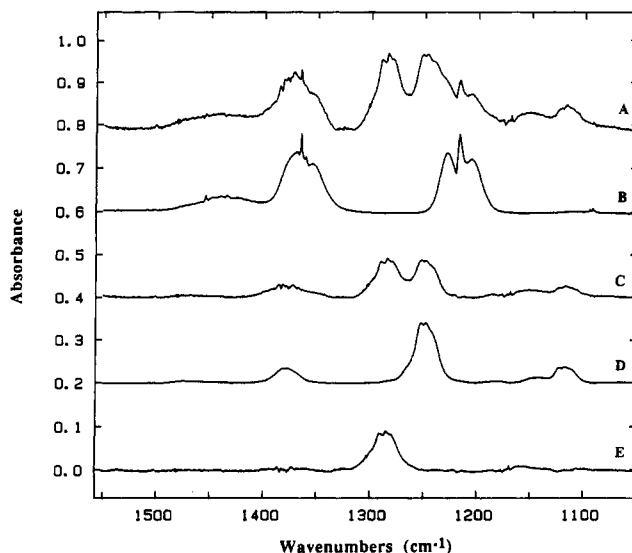


Figure 8. Identification of products from experiments with DIPE. (A) Spectrum of stable products. (B) Reference spectrum of acetone (3.5 ppm). (C) The result of the spectral subtraction of B from A. (D) The reference spectrum of isopropyl acetate (1.0 ppm). (E) The result of the spectral subtraction of D from C; the remaining band arises from isopropyl nitrate.

show that this pathway is of minor importance for the ether destruction by OH. None of these compounds have been observed in our experiments indicating that, in the NO₃ case, attack on the *tert*-butyl side is negligible and that NO₃ is more selective for hydrogen abstraction from the secondary ethoxy carbon.

DIPE. DIPE is a symmetric ether, and the probability of NO₃ attack is equal on both sides of the molecule. However, the oxidation may start either at the primary or at the tertiary C-H site.

In this experiment, acetone, isopropyl acetate (IPA), and formaldehyde were formed in fractional yields of 1.07, 0.31, and 0.31, respectively. Absorption bands at 1653, 1284, and 846 cm⁻¹ were attributed to isopropyl nitrate. The average organic nitrate absorption coefficient (see Table 1) was used to estimate its concentration, resulting in a fractional yield of 0.31. The conversion of DIPE was 22% of the original amount (3.3 ppm). An IR spectrum of the products is presented in Figure 8.

Depending on the site where the degradation of DIPE is started, two separate sets of products will be obtained. Acetone and isopropyl nitrate are formed according to the reaction scheme given in Figure 9 (path I) when the oxidation begins at the tertiary site. The sum of the amounts of acetone and isopropyl nitrate divided by two (the molecule falls apart in two pieces) corresponds to 69% of reacted DIPE. The isopropyl acetate and formaldehyde are formed in equal amounts when the degradation is started at the primary C-H site as is illustrated by path II in Figure 10. The mass balance is excellent; the fraction of products formed in path I and the fraction from path II give together 1.00.

The nitrate radical reacts with DIPE preferentially at the tertiary C-H site. The reactivity of the primary C-H sites is not negligible and represents, in our experiment, about 31% of the total reactivity.

The products of the atmospheric oxidation of DIPE initiated by Cl and OH radicals were studied using FTIR spectroscopy by Wallington et al.⁵ In contrast to our results, isopropyl acetate was reported to form in a 1:1 relation to disappeared DIPE while no acetone was observed. Wallington et al.⁵ ended their experiments when less than 10% of their starting material had been consumed while in this work slightly more than 20% disappeared. Therefore, we have considered the possibility of acetone being formed from a secondary reaction where nitrate radicals attack the hydrogen atom on the secondary carbon in the alcohol residue of isopropyl acetate. After stabilization with

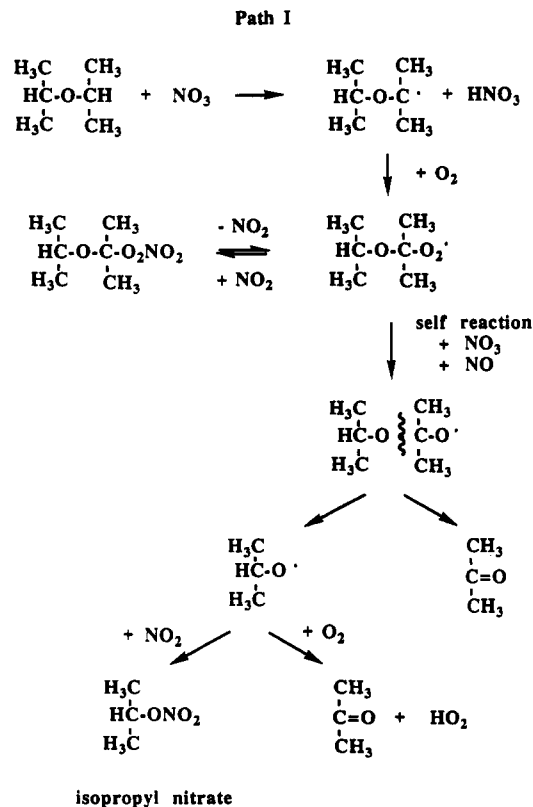


Figure 9. Suggested mechanism for the reaction of the nitrate radical with DIPE leading to the formation of acetone and isopropyl nitrate.

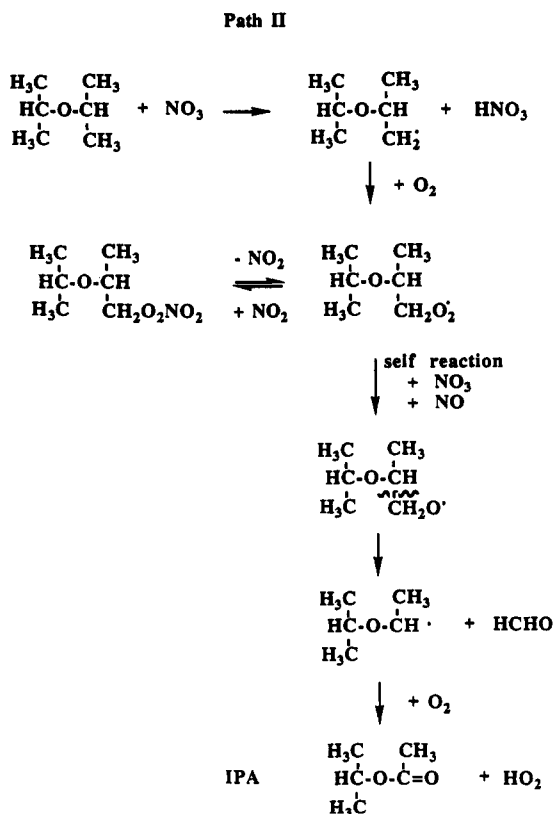


Figure 10. Suggested mechanism for the reaction of the nitrate radical with DIPE leading to the formation of isopropyl acetate and formaldehyde.

molecular oxygen and reduction, the resulting oxy radical would be expected to break up into acetone and an acetoxy radical. The acetoxy radical would thereafter decompose into CO_2 and a methyl radical that subsequently would form formaldehyde. We reject this possibility of a secondary reaction because if acetone originated exclusively from reaction of the isopropyl acetate, then

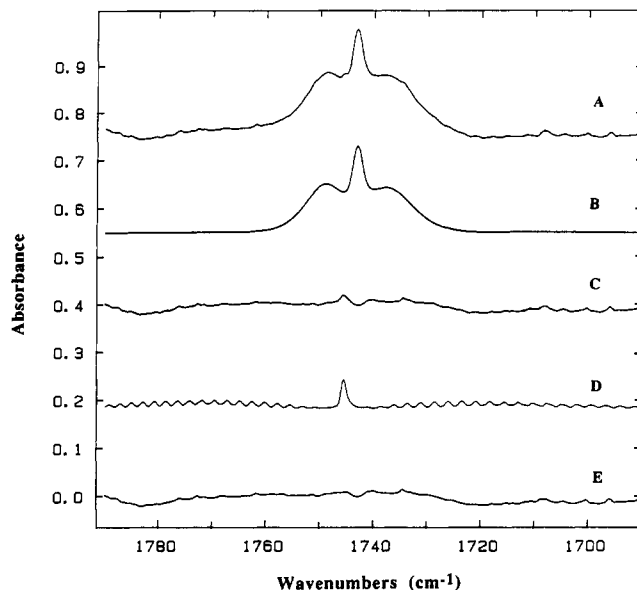


Figure 11. Identification of products from experiments with TAME. (A) Spectrum of stable products. (B) Reference spectrum of *tert*-amyl formate (1.6 ppm). (C) The result of the spectral subtraction of B from A. (D) Reference spectrum of formaldehyde (1 ppm). (E) The result of the subtraction of spectrum D, scaled by a factor of 0.4, from C.

the sum of isopropyl acetate and acetone would be less than or equal the loss of DIPE. In our experiments, this sum is significantly greater than the loss of DIPE. One would also expect to see a CO_2 formation corresponding to the amount of acetone. However, no production of CO_2 could be seen in our spectra. In addition, the NO_3 -isopropyl acetate reaction would require a reaction rate coefficient which would be unexpectedly high¹⁰ to effect efficient breakdown of the isopropyl acetate formed. A possible explanation of the difference between OH and NO_3 reaction products is that the energy distribution between the reaction products from peroxy radical-NO and peroxy radical- NO_3 or HO_2 reaction (cf. Figure 9) differs. Such a difference could result in the oxy radical splitting off a methyl radical after NO reaction, while in the case of NO_3 or HO_2 reaction, the scheme depicted in Figure 9 is followed.

TAME. Consistent with ETBE, the major site of NO_3 attack is on the methoxy side of the ether. The CH_3 and CH_2 groups on the *tert*-amyl side are sufficiently isolated from the influence of oxygen, and their contribution to the rate coefficient can be estimated to be of the same order of magnitude as for the corresponding alkanes.¹⁷ Then the room temperature contribution of the *tert*-amyl group would be $2.3 \times 10^{-17} \text{ cm}^3 \text{ molecule}^{-1} \text{ s}^{-1}$, which represents approximately 1% of the overall TAME rate coefficient of $2.02 \times 10^{-15} \text{ cm}^3 \text{ molecule}^{-1} \text{ s}^{-1}$ at 295 K. However, the most convincing evidence for the preference for abstraction from the methoxy hydrogen atoms is obtained from the product distribution.

The final products observed in our experiments were *tert*-amyl formate (TAF) and HCHO in fractional yields of 0.80 and 0.19, respectively. About 2.0 ppm or 19% of the initial amount of TAME reacted into products. Figure 11 shows the final IR spectrum after NO addition when nitric acid and unreacted TAME have been subtracted. The absorption features at 1667, 1291, and 843 cm^{-1} are attributed to *tert*-amyl nitrate. The fractional yield of this nitrate was 0.21 using an absorption coefficient estimated as described above.

The suggested route to formation of the products can be followed in the reaction scheme in Figure 12. TAME-originated alkoxy radicals, formed in the usual way from alkylperoxy radicals, may be converted to stable products by two processes. Abstraction of a hydrogen atom from the $-\text{CH}_2\text{O} \cdot$ group by molecular oxygen leads to the formation of *tert*-amyl formate (TAF), accompanied

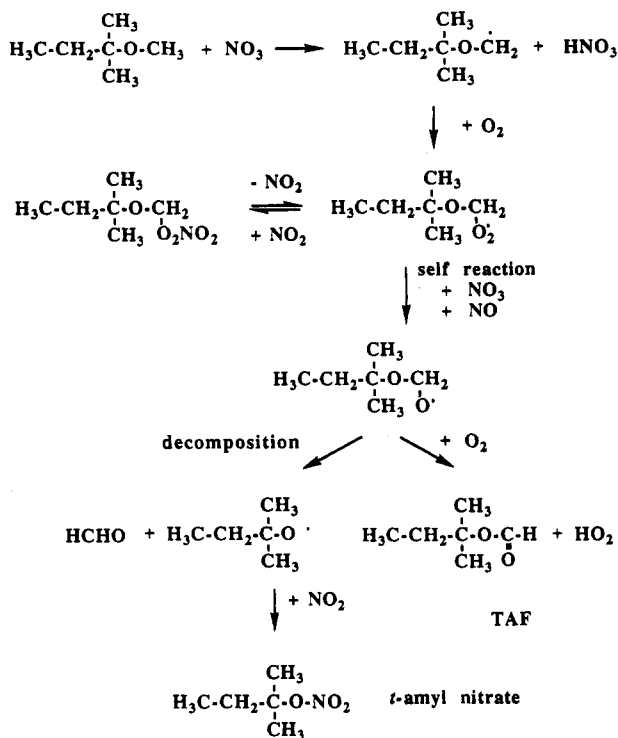


Figure 12. Reaction mechanism for the reaction of the nitrate radical with TAME leading to the formation of *tert*-amyl formate, *tert*-amyl nitrate, and formaldehyde.

by an HO₂ radical. The alkoxy radical can conceivably also be removed by decomposition which leads to formation of HCHO and *tert*-amyl radicals. By subsequent reaction with NO₂, *tert*-amyl nitrate will be formed as the final product. The branching ratios between the reaction with O₂ and the decomposition of the alkoxy radical are given by the fraction of TAF and the fraction of (HCHO + *tert*-amyl nitrate)/2, indicating that about 80% of the alkoxy radicals react with O₂. The mass balance is well closed in these experiments.

Japar et al.¹⁸ and Smith et al.¹⁹ studied the OH and Cl radical initiated oxidation of methyl *tert*-butyl ether (MTBE), which is quite similar to that of TAME. These authors found formaldehyde and *tert*-butyl formate (TBF), which is analogous to the formation of *tert*-amyl formate (TAF) and formaldehyde, as major products. In addition, they also observed methyl acetate and acetone, which is indicative of OH radical reaction on the *tert*-butyl side of MTBE. No corresponding compounds, providing evidence for NO₃ radical reaction on the *tert*-amyl side of TAME, have been observed in our experiments.

Conclusions

The reaction between ethers and nitrate radicals proceeds with rates which are higher than estimated¹⁷ from the corresponding

alkanes having the same number and type of C-H bonds. The products of the atmospheric degradation of the investigated ethers are, in general, structurally related esters, formaldehyde, and organic nitrates. Using rate constants for reaction of the hydroxyl radical with ETBE,²⁰ DIPE,⁵ and TAME⁶ and a daytime concentration of hydroxyl radicals²¹ of $1 \times 10^6 \text{ cm}^{-3}$, the resulting atmospheric lifetimes are 31, 28, and 51 h, respectively. Assuming the nighttime concentration of nitrate radicals²¹ under moderately polluted conditions to be $1 \times 10^9 \text{ cm}^{-3}$, atmospheric lifetimes will be approximately 32, 54, and 137 h for ETBE, DIPE, and TAME, respectively. The generally accepted statement that the hydroxyl radical is by far the most effective atmospheric "detergent" would have to be modified in the case of the ethers. The higher reaction rate coefficients with respect to the hydroxyl radical are compensated by the higher concentration of the nitrate radical in the atmosphere bringing reaction rates and atmospheric lifetimes to be quite similar.

Acknowledgment. VOLVO AB Technological Development is gratefully acknowledged for financial support of this work.

References and Notes

- (1) Guidance on Estimating Motor Vehicle Emission Reductions from the Use of Alternative Fuels and Fuel Blends. Report No. EPA-AA-TSS-PA-87-4, U.S.E.P.A.: Ann Arbor, MI, 1988.
- (2) Alcohols and Ethers: A Technical Assessment of their Application as Fuels and Fuel Components. Publ. No. 4261; American Petroleum Institute: Washington, DC, July 1988.
- (3) Wallington, T. J.; Japar, S. M. *Environ. Sci. Technol.* **1991**, *25*, 410.
- (4) Smith, D. F.; Kleindienst, T. E.; Hudgens, E. E.; McIver, C. D.; Bufalini, J. J. *Int. J. Chem. Kinet.* **1992**, *24*, 199.
- (5) Wallington, T. J.; Andino, J. M.; Potts, A. R.; Rudy, S. J.; Siegl, W. O.; Zhang, Z.; Kurylo, M. J.; Huie, R. E. *Environ. Sci. Technol.* **1993**, *27*, 98.
- (6) Wallington, T. J.; Potts, A. R.; Andino, J. M.; Siegl, W. O.; Zhang, Z.; Kurylo, M. J.; Huie, R. E. *Int. J. Chem. Kinet.* **1993**, *25*, 265.
- (7) Calvert, J.; Pitts, J. N., Jr. *Photochemistry*; Wiley: New York, 1966.
- (8) Atkinson, R.; Carter, W. P. L. *Chem. Rev.* **1984**, *84*, 437.
- (9) Langer, S.; Ljungström, E. *Int. J. Chem. Kinet.* **1994**, *26*, 367.
- (10) Langer, S.; Ljungström, E.; Wängberg, I. *J. Chem. Soc., Faraday Trans.* **1993**, *89*, 425.
- (11) Wängberg, I.; Ljungström, E.; Olsson, B. E. R.; Davidson, J. J. *Phys. Chem.* **1992**, *96*, 7640.
- (12) Atkinson, R.; Plum, C. N.; Carter, W. P. L.; Winer, A. M.; Pitts, J. N., Jr. *J. Phys. Chem.* **1984**, *88*, 1210.
- (13) Aird, R. W. S.; Canosa-Mas, C. E.; Cook, D. J.; Marston, G.; Monks, P. S.; Wayne, R. P.; Ljungström, E. *J. Chem. Soc., Faraday Trans.* **1992**, *88*, 1093.
- (14) Canosa-Mas, C. E.; Smith, S. J.; Waygood, S. J.; Wayne, R. P. *J. Chem. Soc., Faraday Trans.* **1991**, *88*, 3473.
- (15) Wängberg, I. *J. Atm. Chem.* **1993**, *17*, 229.
- (16) Barkenbus, C.; Naff, M. B.; Rapp, K. E. *J. Org. Chem.* **1954**, *19*, 1316.
- (17) Bagley, J. A.; Canosa-Mas, C.; Little, M. R.; Parr, A. D.; Smith, S. J.; Waygood, S. J.; Wayne, R. P. *J. Chem. Soc., Faraday Trans.* **1990**, *86*, 2109.
- (18) Japar, S. M.; Wallington, T. J.; Richert, J. F. O.; Ball, J. C. *Int. J. Chem. Kinet.* **1990**, *22*, 1257.
- (19) Smith, D. F.; Kleindienst, T. E.; Hudgens, E. E.; McIver, C. D.; Bufalini, J. J. *Int. J. Chem. Kinet.* **1991**, *23*, 907.
- (20) Wallington, T. J.; Andino, J. M.; Skewes, L. M.; Siegl, W. O.; Japar, S. M. *Int. J. Chem. Kinet.* **1989**, *21*, 993.
- (21) Finlayson-Pitts, B.; Pitts, J. N., Jr. *Atmospheric Chemistry*; Wiley: New York, 1986.